Development of an Active 6-Year-Old Child Human Body Model for Simulation of Emergency Events

(article starts on next page)

Development of an Active 6-Year-Old Child Human Body Model for Simulation of Emergency Events

Karin Brolin[1], Isabelle Stockman[1], Hariharan Subramanian[2], Laure-Lise Gras[1], Jonas Östh[1]

[1.] Chalmers University of Technology, Gothenburg, Sweden. [2.] Indian Institute of Technology, Delhi, India.

Abstract One contributing factor to head injury in restrained child occupants is pre-crash maneuvers and active child human body models (HBMs) can be useful tools to design pre-crash interventions with child safety in focus. This paper implemented postural control in the MADYMO human facet occupant model of a 6-year-old child using feedback controlled torque actuators. Control parameters were tuned and the active HBM was compared to experimental data from braking and steering events with child volunteers. The head and sternum displacements of the active HBM were within one standard deviation of the experimental data, while the original HBM did not capture the volunteer kinematics at all. By predicting biofidelic child kinematics, the developed model shows potential as a useful tool for the automotive industry to study the protective properties of restraint systems in pre-crash scenarios. For autonomous steering events, it was illustrated that the shape of the acceleration pulse highly influences the peak head displacements of child occupants. This is an aspect that needs to be considered when autonomous interventions are designed, to ensure the safety of short forward facing child occupants.

Keywords child, emergency event, human body model, pediatric, postural control.

I. INTRODUCTION

The protection of children in vehicles has improved as a result of increased restraint use by children. Nevertheless, studies show that although children are restrained, injuries still occur [1-3]. Head impacts to the front seat back have been identified as one predominant cause of injury for rear seated, seat belt restrained children in frontal impacts [1-3]. Especially younger children adopt a great variety of postures during a car journey [4-8], which could explain some of the injuries that occur in crash situations. Another major contributing factor to head injuries for restrained children is vehicle maneuvers prior to impact [1-3]. The occupant motion, prior to impact, placed the occupant in a sub-optimal restraint condition allowing head contact with the side interior and the back of the front seat. This is supported by child volunteer data from evasive steering events that showed that rear seated children obtained postures that could potentially lead to poor interaction with the seat belt, even though secured in approved child safety devices [9]. For 4 to 6 year-old children, shoulder belt slip-off occurred in almost 67% of the evasive steering events, while for older children belt slip-off did not occur. Consequently, this indicates that current restraint systems have the potential for further improvement and to reduce injuries further, child protection and restraint systems need to be evaluated for the whole crash sequence, including pre-crash maneuvers. Likewise, future autonomous interventions should be designed and assessed with the child occupant in mind.

Traditionally, Anthropomorphic Test Devices (ATDs) have been used to evaluate safety systems in crash loading. However, for pre-crash loading, ATDs are not suitable to capture the occupant's kinematic responses [10-11]. Volunteer testing can be cumbersome to perform, and in addition volunteers may not be subjected to injurious loads and neither assessment in certification nor regulation can be based on volunteer testing. Hence, the automotive industry needs other tools for development of future restraint systems, as well as safety assessment during the whole crash sequence. In recent years, numerical Human Body Models (HBMs) have become increasingly popular to simulate both pre-crash and in-crash occupant responses. Published child HBMs have been developed for crash scenarios and the limited validation focuses only on crash loading [12]. To study

K. Brolin (+46 (0)31 7721509, karin.brolin@chalmers.se) is Associate Professor, I. Stockman is Ph.D. student, J. Östh is Researcher at Chalmers University of Technology in Gothenburg, Sweden. L.L. Gras was post-doc at Chalmers University of Technology and is now Assistant Professor at Université Claude Bernard Lyon 1, Lyon, France. H. Subramanian is Ph.D. student at the Indian Institute of Technology in Delhi, India.

child occupants' responses during emergency and pre-crash events, it is necessary to implement muscle activity or postural control in the child HBMs and validate the models in the pre-crash loading regime. To date, this has only been done for adult 50th percentile male models [13-14].

The aim of this paper is to implement postural control in a multi body HBM of the 6-year-old child, tune and validate its responses to child volunteers' in braking and steering emergency events, and test the HBM in an application to study how the shape of a lateral acceleration changes its kinematics. The developed active child HBM has the potential to contribute to child safety related restraint concepts studies to maintain the child in a beneficial position during pre-crash events and autonomous interventions. Thereby, it contributes to improve the protective capacities of the vehicle, safety systems and child restraints in the whole crash sequence.

II. METHODS

Postural control was implemented for the MADYMO human facet occupant model of a 6-year-old child version 2.2 [15] (6YO HBM) with feedback control of the spinal and hip joints as described below. The model with postural control is hereafter called the 6YO HBM with PC. The control parameters were tuned to child volunteer experiments with braking and steering events [9, 16]. Then, the 6YO HBM with PC was evaluated in gravity loading and validated to another volunteer experiment with steering events [17]. Finally, the 6YO HBM with PC was applied to study how the shape of a lateral acceleration pulse changes the lateral movement. MADYMO Release 7.4.1 code (TASS, Rijswijk, the Netherlands) was used for all simulations and post processing was done using MATLAB version R2010b (MathWorks, Natick, Massachusetts, USA).

The Child Model

The 6YO HBM has a stature of 116 cm and weighs 21 kg. It was scaled-down from the adult 50th percentile male model in terms of geometry and for most of the mechanical properties, as described in [15]. Briefly, it consisted of 92 bodies. In the spine, each vertebra was a separate rigid body connected to the neighboring vertebra by free joints with lumped joint resistance. (Fig. 1). The thorax and abdomen were composed of flexible bodies, the skin and the pelvis of facet elements, and the shoulders as well as lower and upper limbs were a combination of rigid bodies and joints. No modifications were done to the 6YO HBM during implementation of postural control; hence all the mechanical properties were kept the same.

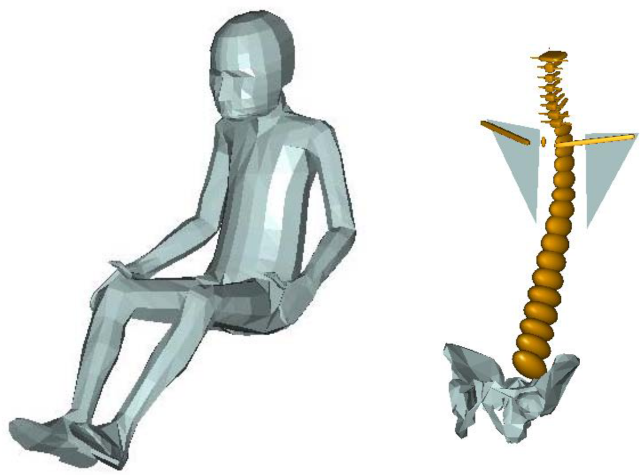

Fig. 1. The 6YO HBM [15] and its spine.

Experimental Data

Three sets of experimental child volunteer data (Table 1) were used in this study for the purpose of model comparisons; a braking event with approximately 1 g deceleration [16], a steering event with approximately 0.8 g lateral acceleration [9], and a steering event with approximately 0.6 g lateral acceleration [17]. The study protocols were reviewed and approved by The Ethics Board of Gothenburg, Sweden. Fig. 2 illustrates the three acceleration pulses. All three emergency events were performed on a test track in a Volvo XC70 car [9, 16-17]. Volunteers were seated on a booster cushion on the right rear seat of the vehicle and restrained by the standard three-point seat belt. Vehicle data was collected and synchronized with video data. For the braking and 0.8 g steering events, four cameras (Monacor TVCCD-30, lens focal length 3.6 mm) with a recording rate of 12.5 frames per second were used and provided one frontal, one lateral, and two oblique views of the child volunteers. For the 0.6 g steering event, two color cameras (UI-5220CP-C Gigabit Ethernet CMOS, IDS GmbH, Obersulm, Germany) with wide angle lenses (LM5NCL, Kowa Co., Tokyo, Japan) and with a recording rate of 50 frames per second were used and provided one frontal and one lateral view of the child volunteers (lens focal length 3.5 mm and 4.5 mm, respectively). Volunteer kinematic responses were determined from continuous video tracking of markers and anatomical landmarks on the children. For the braking event, continuous data were available for the forehead marker and ear. For the 0.8 g steering event, kinematic data for the nasion and sternum marker was only available at three points in time: one reference point and at two intervals (T2 and T3) during the initial part of the steering event [9]. At the point T2 the vehicle had moved a distance that can be considered a reasonable distance to move laterally to avoid an impact with an approaching vehicle. At the point T3 the motion of the vehicle could simulate a situation where the vehicle has managed to avoid the first event but then impacts something else. For the purpose of this paper, data collected at 0.6 s (at the end of the ramping phase of the acceleration pulse, T3 in [9]) was used since it was assumed to be closest to the maximum displacement. For the 0.6 g steering event, the kinematic data for the nasion and sternum markers at the time of maximum lateral displacements of the child volunteers were used.

TABLE 1
VOLUNTEER DATA COMPARED TO THE 6YO HBM, MEAN (STANDARD DEVIATION).

	0.8 g Steering and 1 g Braking [9, 16]	0.6 g Steering [17]	6YO HBM [15]
Number of volunteers	8	10	-
Age [years]	5.3 (1.0)	5.5 (0.6)	6
Stature [cm]	117 (6)	114 (3)	116
Seated height [cm]	59 (3)	66 (3)	63
Weight [kg]	20 (3)	20 (2)	21

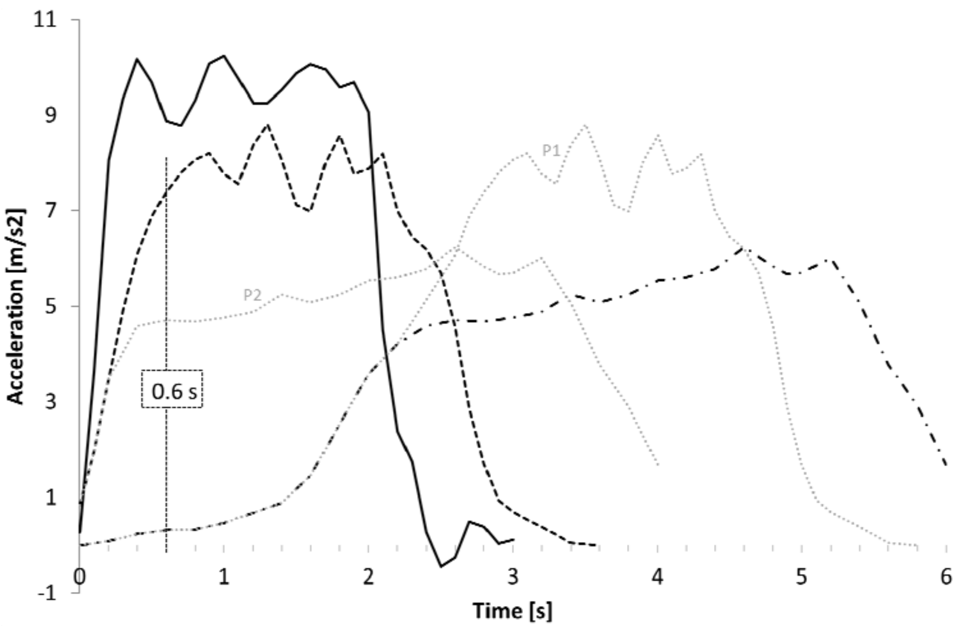

Fig. 2. Acceleration as function of time for the three experiments: deceleration in the braking event [16] (solid line), lateral acceleration in the 0.8 g steering event [9] (dashed line), and lateral acceleration in the 0.6 g steering event [17] (dash-dotted line); and the two created lateral accelerations P1 and P2 (grey dotted lines). The vertical dash line indicates the point in time (T3 in [9]) where data for the 0.8 g steering event were collected.

Setting up the Models

To simulate the volunteer experiments, models of the booster cushion, the rear seat and three-point seat belt were created. The booster cushion model (Britax Ranger) was previously published in [18] (Fig. 3). The rear seat was simplified with two planes: a 42-by-45 cm plane for the seat cushion with a 10° angle to the car floor and a 55-by-45 cm plane for the seat back. The angle between the seat cushion and the seat back was 100° to reproduce the geometry of the rear seat in the test vehicle. The coordinate system of the vehicle model had the X-axis pointing forward, Y-axis to the left, and Z-axis upward (Fig. 3).

The three-point seat belt was modelled by FE and MB elements with insertion points corresponding to the right rear seat of the test vehicle. The MB elements connected the FE belt to the belt anchorages, and the triangular membrane FE elements modelled the interaction between the belt and the HBM. The lap belt's anchorages were placed at the junction of the seat back and seat cushion (5 cm from the seat cushion right and left sides; Fig. 3 D,G). The shoulder belt's lower anchorage was the same as the right lap belt's anchorage, while the upper anchorage was placed 60 cm above and 23.5 cm behind the left side of the seat back-to-seat cushion junction (Fig. 3 B), intermediate points attached under the guiding loops of the booster were added to guide the belt (Fig. 3 C,E,F). Friction of 0.3 was used for all intermediate belt nodes and the buckle, allowing belt slip between the shoulder and lap belts. A retractor was defined for the shoulder belt with belt slip that was tuned for sternum forward displacement in the braking event (0 mm - 0 N, 13 mm - 13 N, 54 mm - 50 N, 55 mm - 1050 N). After positioning the model, the seat belt was routed along the facet skin elements of the 6YO HBM using the belt fitting tool available in XMADGic (TASS, Rijswijk, the Netherlands). The shoulder belt was positioned mid-shoulder (Fig. 4).

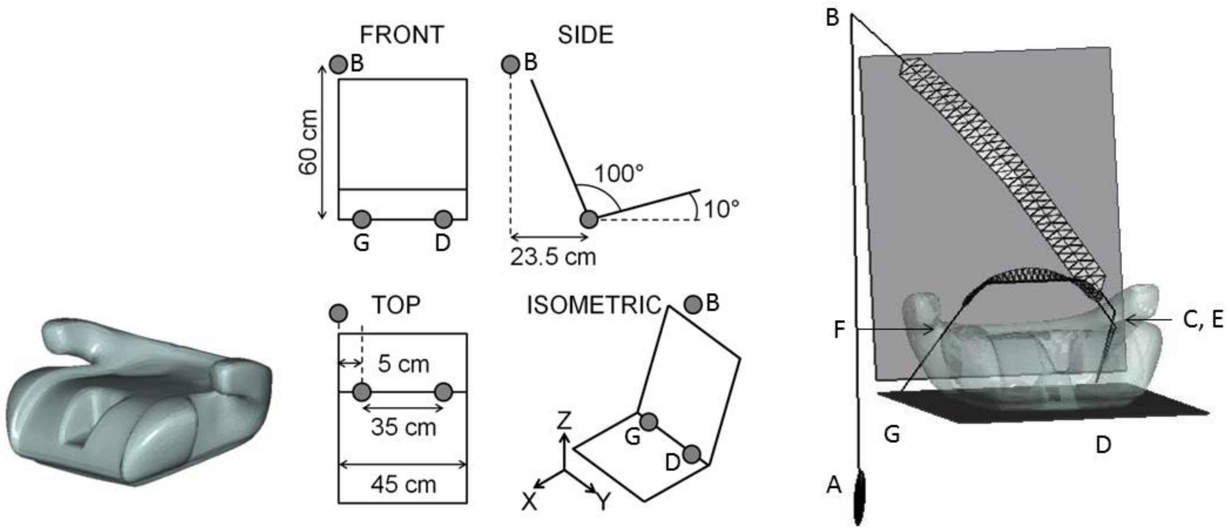

Fig. 3. Model of the booster cushion (left), schematic illustration of the rear seat geometry and belt insertion points (middle), and the combined models of the rear seat, booster and seat belt (right). A: Retractor. B: Shoulder belt anchorage. C, E, and F: Intermediate points to guide the belt under the guiding loops of the booster. D: Buckle. G: Lap belt anchorage.

Contacts were defined between the booster and the rear seat, the facet skin of the 6YO HBM and the rear seat, the facet skin of the 6YO HBM and the booster, the facet skin of the 6YO HBM and the FE belt elements. Friction of 0.3 was defined for all contacts except the booster to rear seat where 0.55 was used to compensate for the lack of seat curvature. The contact characteristics were governed by the 6YO HBM contact characteristics for all contacts with the 6YO HBM.

An initial static simulation was performed with gravity loading to position the models such that contact force equilibrium was reached. For this simulation, all spinal joints of the 6YO HBM were locked. The 6YO HBM was positioned right above the booster cushion that was positioned right above the rear seat, both models centered over seat. Gravity was applied and the simulation duration was 4 seconds to ensure that all models were in contact and any oscillations had diminished (Fig. 4). The hands of the 6YO HBM were positioned at the end of the guiding loops of the booster. Nodal points on the skin of the 6YO HBM were tracked for the volunteer measurements at the nasion, forehead, upper and mid sternum locations (Fig. 4).

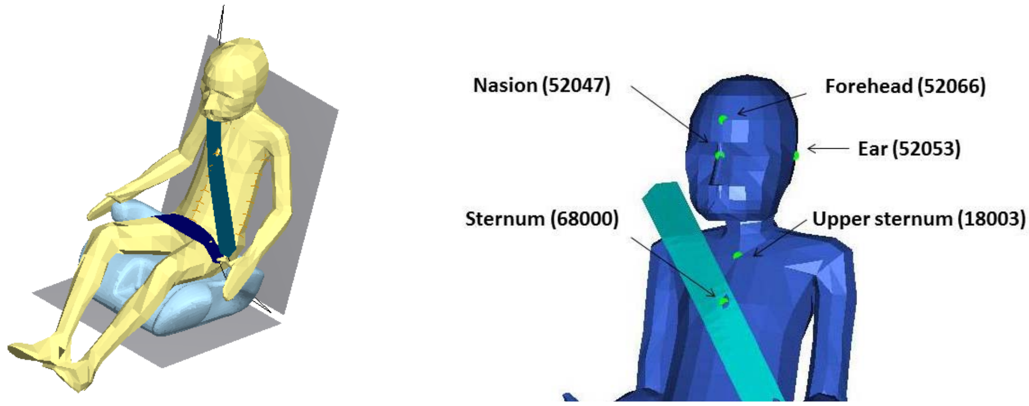

Fig. 4. Model set-up for simulation of volunteer experiments after positioning and belt fit and the nodes tracked for comparison to volunteer data.

Implementation of Postural Control

Postural control was implemented with 81 feedback controlled torque actuators, at each spinal joint and the hip joints. All the three rotational degrees of freedom were controlled separately; for the spinal joints: flexion-extension, lateral bending, and axial rotation, and for the hip joints: flexion-extension, abduction-adduction, medial-lateral rotation. The torques applied by the actuators were divided into two components: static and dynamic torques. The static torque was applied to maintain the initial position of the child model and calculated in a separate static simulation where all spinal joints were locked and only gravity load applied to the model. The dynamic torque was calculated with Proportional, Integral, and Derivative (PID) feedback control to change the applied torque in the actuator when a disturbance of the model's posture occurred. Posture was monitored at each joint and the controllers used signals from sensors measuring the angle of the distal rigid body relative to the global frame of reference. The postural control was implemented in a separate input file so that the 6YO HBM easily can be used with or without the postural control and to allow for the postural controllers to be used with later releases of the 6YO HBM.

The control parameters were adapted from values used for adults found in the literature [13-14]. The derivative and integral time constants were set to 0.1 s and 1 s, respectively [13]. The controller gains were taken from [14] and, to provide a starting point, reduced by half to represent a 6-year-old child (6YO HBM with PC 1st set of control parameters). Then, the proportional gains were tuned to experimental data by iteratively changing the proportional gains in increments of 10% of the adult value in [14] until the nodal response of interest was within the experimental corridors. The same values were used for all three rotational degrees of freedom. The tuning was performed in two steps:

1. The proportional gains for the cervical spine were changed in simulations of the braking event where the displacement of the forehead node was compared to data from [16], starting with the 6YO HBM with PC 1st set of control parameters and resulting in the 6YO HBM with PC 2nd set of control parameters.
2. The proportional gains for the thoracic and lumbar spine were changed in simulations of the 0.8 g steering event where the displacement of the sternum node was compared to [9], starting with the 6YO HBM with PC 2nd set of control parameters and resulting in the 6YO HBM with PC 3rd set of control parameters.

Simulations

For each simulation, the experimental braking or steering accelerations (Fig. 2) was applied to the seat model, and gravity was applied to the whole system. The 6YO HBM with PC was simulated with gravity only for the first 0.3 s, before applying the acceleration, to ensure a stable seated posture. When compared with the experimental data the model position at time 0.3 was considered as the initial seated posture of the 6YO HBM with PC.

Simulations were performed with the 6YO HBM and three versions of the 6YO HBM with PC in four load cases: gravity loading, a braking event [16], and two steering events [9, 17] (Table 2). The braking event was simulated with the 1st set of control parameters to tune the feedback control parameters for the actuators in the cervical spine by comparing the ear and forehead displacements, providing a 2nd set of control parameters.

Then, the 0.8 g steering event was simulated with the 2nd set of control parameters to tune the feedback control parameters for the actuators in the thoracic and lumbar spine by comparing to the sternum displacement, providing a 3rd set of control parameters. The 6YO HBM with PC and with the 3rd set of control parameters was simulated in a gravitational field only for 3 s, to make sure that it kept its posture over time, and in the braking event for reference. For validation, the 0.6 g steering event was simulated and the displacements of the sternum and nasion were compared to the experimental data [17]. The 6YO HBM without postural control was simulated in all four load cases for reference. To simulate a child holding on to the guiding loops of the booster during the steering events, all simulations were re-run a second time when the hands of the 6YO HBM with PC were constrained to the guiding loops of the booster with point restraints (failure force of 100 N).

Lastly, the 6YO HBM with PC (3rd set of control parameters and point restraints for hands-booster) was used to study lateral acceleration pulses with varying acceleration rate. The acceleration pulses P1 and P2 (Fig. 2) were created by combining the acceleration pulses for the 0.6 g and 0.8 g steering events, such that the beginning of one pulse was used together with the peak acceleration of the other.

TABLE 2
PERFORMED SIMULATIONS, 6YO HBM VERSIONS AND LOAD CASES

	Gravity Only	1 g Braking	0.8 g Steering	0.6 g Steering
6YO HBM	For reference	For reference	For reference	For reference
6Y0 HBM with PC 1st set	-	To tune 2nd set	-	-
6Y0 HBM with PC 2nd set	-	x	To tune 3rd set	-
6Y0 HBM with PC 3rd set	Stability analysis	For reference	x	Comparison

- : No simulation performed for this combination of model and load case. x: Simulation results from a tuning.

III. RESULTS

Tuning of the 6YO HBM with PC for a braking and a steering event resulted in the set of control parameters listed in Table 3, where the proportional gains in the cervical spine were reduced and in the thoracic and lumbar spine were increased, compared with the original model, to provide a model response within the experimental corridors [9, 16]. Fig. 5 provides visual comparisons of the maximum displacements for this improved version of the 6YO HBM with PC and volunteers from the experimental braking, 0.8 g and 0.6 g steering events [9, 16-17]. The shoulder belt did not slip off in the simulation of the braking event, but slipped off the shoulder in both the 0.8 g and 0.6 g steering events (after 0.35 and 2.1 s respectively). When the 6YO HBM with PC had point constraints between the hands and the booster, head displacement was slightly decreased: 0.7 cm, 2.1 cm, and 1.8 cm for the braking, 0.8 g and 0.6 g steering simulations, respectively.

TABLE 3
3RD SET OF CONTROL PARAMETERS FOR THE 6YO HBM WITH PC

Body Region	Joints	Proportional Gains [Nm/rad]			
		Flexion-Extension	Lateral Bending Abduction-Adduction	Axial & Medial-Lateral Rotation	Adult [14]
Cervical Spine	Head / C1 to C6 / C7	4	4	4	20
Thoracic Spine	C7 / T1 to T11 / T12	30	30	30	50
Lumbar Spine	T12 / L1 to L5 / Sacrum	45	45	45	75
Hip	Upper leg / pelvis	37.5	37.5	10	-

The 6YO HBM did not maintain its posture in the gravity field and fell over with the head toward the floor of the vehicle. The 6YO HBM with PC did maintain a stable posture with time, and the tracked node on the head had a maximum displacement less than 1 cm rearward during the first 0.25 s and then moved toward a stable head location approximately 0.3 cm rearward and 0.5 cm downward from the starting position.

For the braking event, the 6YO HBM with PC (all sets of control parameters) correlated well with the volunteer data for the X- and Z-head displacements measured for the ear marker (Fig. 6A). If postural control was not included the 6YO HBM behaved differently than the child volunteers, with very large forward and downward displacement of the sternum and head. For the 1st set of control parameters the head rotation was too small and therefore the head displacement measured at the forehead was outside the volunteer corridors. Reducing the proportional gain in the cervical spine resulted in greater neck flexion and head rotation, so that the 2nd set of control parameters for the 6YO HBM with PC provided a good correlation to both ear and forehead kinematics (Fig. 6A). Tuning of the thoracic and lumbar spine control parameters had a small impact on the response of the 6YO HBM with PC in the braking event, as can be seen by the two curves almost overlapping in Fig. 6A.

For the 0.8 g steering event, the 6YO HBM with PC moved predominantly to the side rather than downward, as was the case without postural control (Fig. 6B). The 6YO HBM with PC and the 2nd set of control parameters moved just outside the sternum experimental range of motion at 0.6 s (T3 in [9]) and with the 3rd set of control parameters the sternum displacement of the HBM was still larger than the mean displacement of the volunteers, but within the experimental ranges. The head displacement measured at the nasion node compared well to the mean experimental value for the 6YO HBM with PC and the 3rd set of control parameters. The two versions of the 6YO with PC moved very similarly, the main difference being the magnitude of displacements.

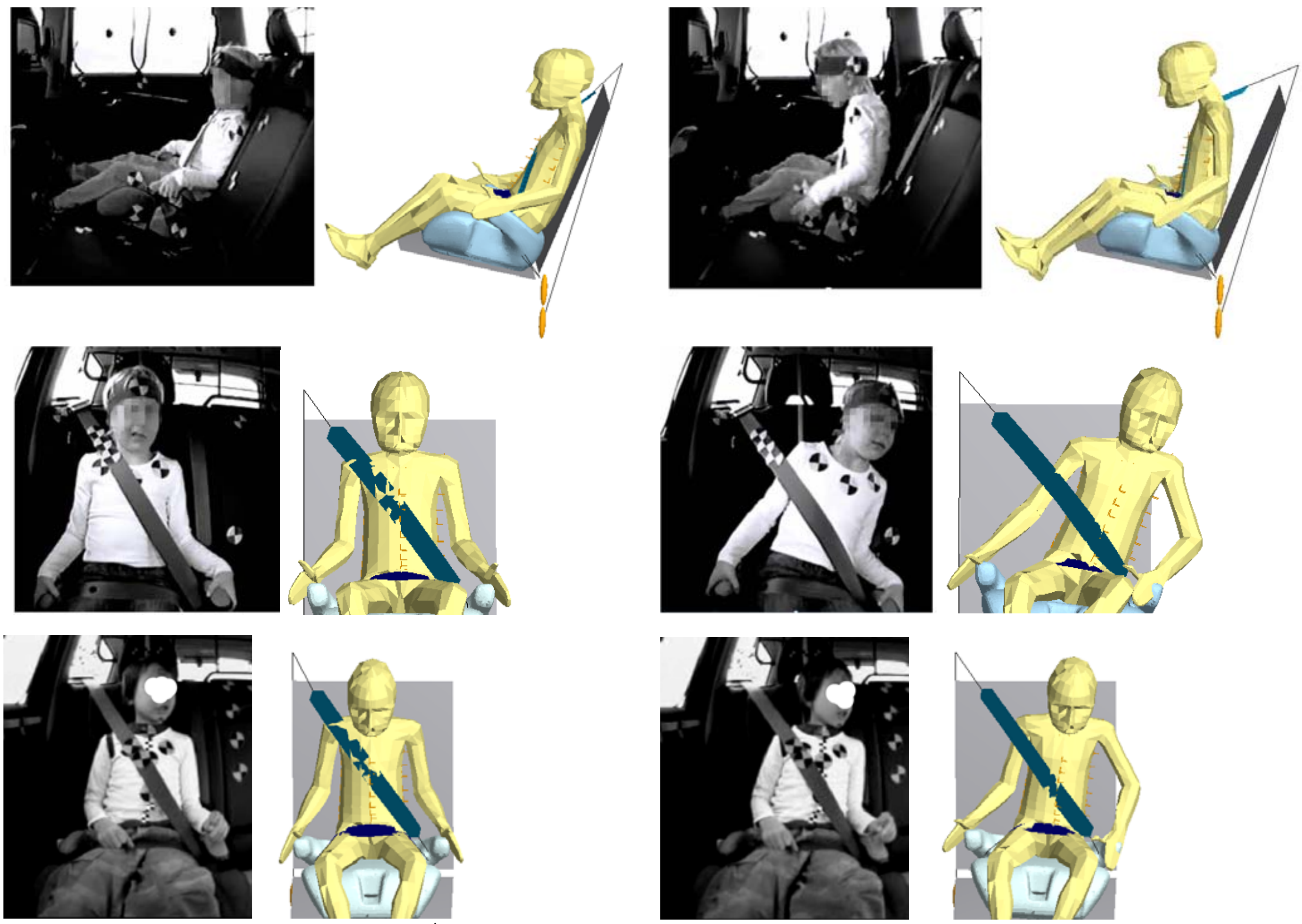

Fig. 5. The 6YO HBM with PC (3rd set of control parameters and point restraints for the hands-booster) compared to volunteers at start and at maximum head displacement for the braking event [16] (top row), the 0.8 g steering event [9] (middle row), and 0.6 g steering event [17] (bottom row).

The 6YO HBM with PC (3rd set of control parameters) compared very well to the 0.6 g steering event [17] (Fig. 7). The head, measured at the nasion, moved in the horizontal plane until the rebound. The maximum head lateral displacement was larger than the experimental mean value but within one standard deviation of the experimental data. Similarly, the sternum displacement was almost horizontal until the maximum value and then rebounded with an upward movement.

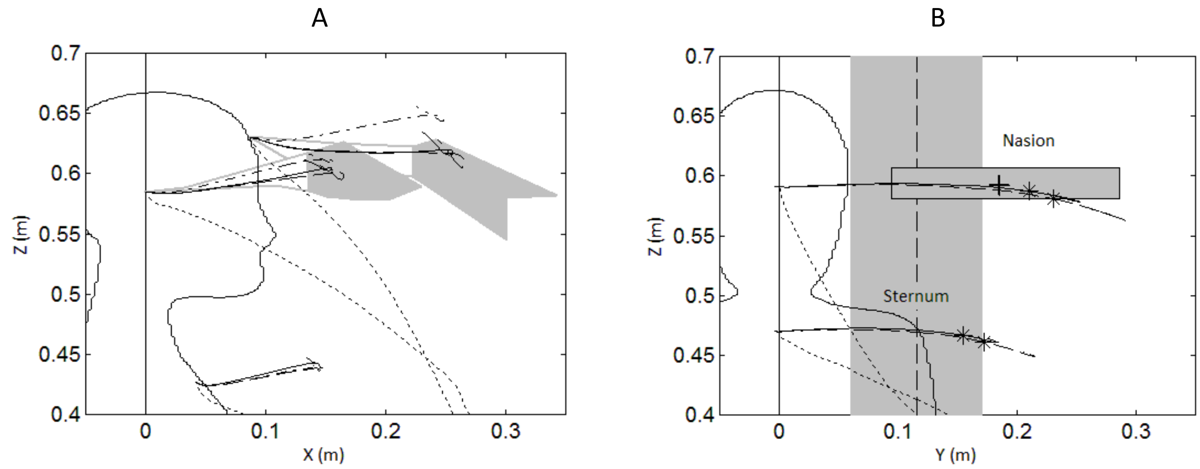

Fig. 6. Nodal displacements compared to experimental braking (A) and 0.8 g steering (B) for different versions (hands were free to move); 6YO HBM (dotted line in A & B), 6YO HBM with PC 1st set of parameters (dash-dotted line in A), 6YO HBM with PC 2nd set of parameters (dashed line in A & B), and 6YO HBM with PC 3rd set of parameters (solid line in A & B). Volunteer and 6YO HBM data are normalized to the same seated height. A: The braking event [16] with the envelope of the experimental displacements of the forehead and ear targets illustrated by grey lines and the maximum forward displacements by the filled grey area. B: The 0.8 g steering event [9] with the experimental displacements at time T3 (0.6 s); the mean sternum X-displacement (vertical dashed line) and the range of X-displacements as corridors in grey, and the nasion range of X- and Z-displacements (grey box with black outline) and mean value (+). The simulations results at 0.6 s are marked with stars (*).

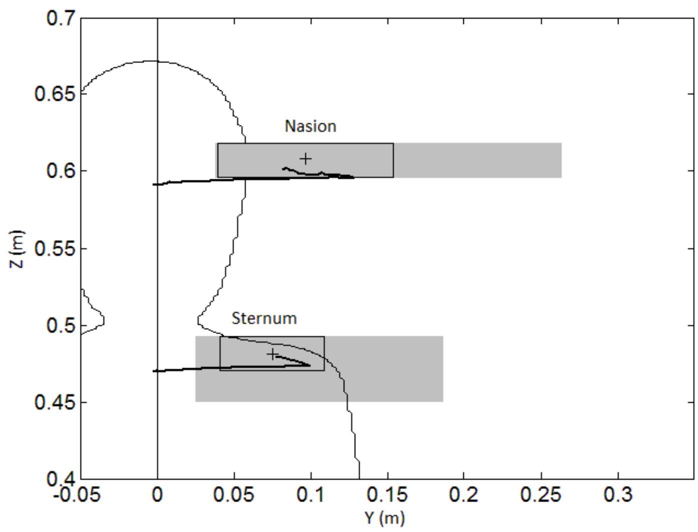

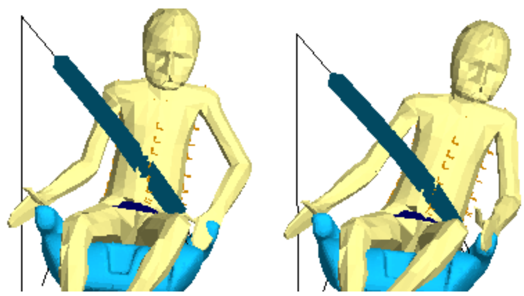

Fig. 7. Nasion and sternum displacements for the 6YO HBM with PC 3rd set of parameters (solid line) compared to 0.6 g steering event [17]: maximum experimental sternum and nasion displacement mean value (+), standard deviation (grey box with black outline) and range of experimental data (grey box without outline) [17]. Volunteer and 6YO HBM data are normalized to the same seated height.

Fig. 8. Maximum displacement and belt slip-off for the 6YO HBM with PC for the simulations with lateral acceleration P1 (left) and the 0.8 g steering event (right).

Applied to study the influence of the shape of the lateral acceleration pulse, the 6YO HBM with PC illustrated that not only the peak acceleration but also the slope of the acceleration curve changes the kinematics (Table 4). The created pulse P1 compared with the simulations of the 0.8 g steering event decreased head and sternum lateral displacements with 9.1 and 5.4 cm, respectively (Fig. 8). The created pulse P2 compared with the simulations of the 0.6 g steering event increased head and sternum lateral displacements with 4.0 cm and 2.5 cm, respectively.

TABLE 4
INFLUENCE OF THE SHAPE OF THE LATERAL ACCELERATION PULSE IN STEERING EVENTS.

Acceleration pulse	0.6 g Steering	P2	0.8 g Steering	P1
Maximum acceleration [g]	0.6	0.6	0.8	0.8
Approximate time until 0.3 g [s]	1.9	0.2	0.2	1.9
Maximum nasion displacement [cm]	11.3	15.3	23.4	14.3
Maximum sternum displacement [cm]	8.7	11.2	16.9	11.5

IV. DISCUSSION

We have implemented postural control in a multi body HBM of the 6 year-old child through feedback control. Initial values for the control parameters were taken from an adult model [14] and tuned so that the kinematic response of the 6YO HBM was within the experimental ranges of two volunteer test conditions subjecting children to braking and steering events [9, 16]. The 6YO HBM with PC was validated to another steering event [17] with acceptable correlation; the kinematic response of the model was within one standard deviation of the child volunteer data. It should be noted that the original 6YO HBM could not predict the child volunteer responses in any of the three emergency events and should not be used to study pre-crash maneuvers. Lastly, the 6YO HBM with PC was applied to study the influence of the shape of the lateral acceleration pulse on the sideward movement in a steering event. The two pulses with a peak acceleration of 0.8 g both had belt slip-off from the shoulder but the sideward head displacement was much lower when the acceleration was ramped up slower, illustrating that the initial shape of the acceleration pulse in an autonomous event does influence the protective capacity of the child restraint system. This application illustrates the potential usefulness of the 6YO HBM with PC as a tool to develop and assess the child safety of integrated safety systems and autonomous interventions.

The original 6YO HBM was the MADYMO human facet occupant model of a 6-year-old child version 2.2 [15]. Its geometry was scaled down from the male adult model with separate scaling factors for the three axis of each body part, based on a target geometry from the CANDAT database with child anthropometries [15]. Similarly the mass and moments of inertia were scaled down to represent a 6-year-old child. We consider the main limitations of the 6YO HBM to be the lack of; 1) age dependent material properties and 2) validation for crash loading scenarios. Hence, there is more work needed before pre-crash simulations can be combined with reliable in-crash simulations.

In the human body, postural control is an involuntary feedback control process in which the central nervous system utilizes, for instance, muscle spindle stretch reflex mechanisms and the golgi tendon organs for the limbs [19] and the vestibular organs of the ear for the head and neck [20-21]. In addition, voluntary movements with muscle activation schemes based on past experience are superimposed in normal human motor control [22]. Therefore, capturing the postural response of car occupants, children or adults, in a mechanical or mathematical model presents a large challenge. In particular, overall mechanical resistance of the joints in the body will change in the order of magnitudes as muscles spanning the joint increase their activity. We used a feedback control approach to simulate postural control in the 6YO HBM with PC. Two main reasons make this modeling approach suitable; 1) its resemblance of actual human postural control in which the nervous system utilizes feedback control, and 2) it has the potential to represent a large range of mechanical properties of the joints in the model. Nonetheless, some limitations are inherent in the present modeling approach. First, torque actuators on the joint level were used rather than muscle elements as done by [13, 23] or a continuum muscle model as in [24]. Second, muscle activation dynamics [25] and neural delays are not included in the feedback loops for the regulators. Hence, the torque actuators will respond to a disturbance faster than the human neuromuscular system will respond.

The proportional control gains were assumed to be equivalent for all three degrees of rotation, which may not be the case and should be further investigated. Also, the gains were assumed to be equivalent for all controllers in the cervical, lumbar and thoracic regions, respectively. Thereby reducing the number of variables that were changed during the tuning of the spinal gains, from 75 to 3. This limitation ensured consistent gain values along the length of the spine and was necessary since the experimental child kinematics were analyzed only at a limited number of anatomical points. It makes sense from a biomechanical point of view that the controller gains decrease from the head toward the lumbar spine since the muscle strength of the inferior spine increases to control a larger mass of the superior body. The tuning process was straight forward in the sense that the first set of values that were within the experimental corridors was picked. Hence, there is probably a potential to optimize the response further, providing that there is more detailed experimental data in terms of the number of measured points on the body of the child. Despite these limitations, the 6YO HBM with PC was able to obtain postural control kinematics similar to child volunteers.

The controllers use joint angle with respect to the global reference frame for all spinal controllers to calculate the actuators' torque. This means that each spinal controller will try to maintain its orientation in space, which appears to work well for the application to pre-crash simulations. This control strategy is essentially a head-in-space strategy, which is suitable for low frequency perturbations [20] such as the braking and steering interventions modeled here. The same approach has been hypothesized for the postural control of braking motorcycle drivers [26].

Based on the results from the volunteer study in [9] it can be assumed that 10 to 12 year-old children are in a more stable restraint situation in steering maneuvers than the shorter 4 to 6 year-old children. This is most likely due to anatomical differences in combination with muscle properties and maturity. Short children in an unstable restraint situation during a pre-crash maneuver need more support from restraint systems or the vehicle. Therefore, an HBM of the 6 year-old had the highest priority. In the steering events [9, 17] the shoulder belt slipped off more than 60% of the children, which is in accordance with the 6YO HBM with PC simulations here. The belt slip off was more pronounced in the simulations of the 0.8 g steering event than in the 0.6 g steering event. This is likely explained more by the slower acceleration rate in the 0.6 g steering event than by the difference in peak acceleration level, which is supported by a simulation where the shape of the acceleration curve from the 0.6 g steering event was used with a peak acceleration of 0.8 g that decreased the inboard head displacement by 9 cm. Future autonomous interventions may be more aggressive than 0.8 g peak acceleration and to ensure the safety of children that may end up in less beneficial positions during these maneuvers, we recommend that this issue is studied in more depth and especially considered in the development of autonomous steering and other avoidance maneuvers with lateral loading components.

V. CONCLUSIONS

Postural control was implemented in MADYMO human facet occupant model of a 6-year-old child using feedback controlled torque actuators in the spinal joints. The control parameters were tuned to volunteer data from 1 g braking and 0.8 g steering events. The 6YO HBM with PC could maintain a stable posture with gravity loading and its head and sternum kinematics was within one standard deviation of volunteer responses in 0.6 g steering events. The developed model shows potential as a useful tool for the automotive industry to study the protective properties of restraint systems in pre-crash scenarios by predicting biofidelic child kinematics.

For autonomous steering events, it was illustrated that the shape of the acceleration pulse highly influences the peak head displacement of child occupants. This is an aspect that needs to be considered when autonomous interventions are designed to ensure the safety of short forward facing occupants.

VI. ACKNOWLEDGEMENT

The authors would like to thank Lotta Jakobsson (Volvo Cars), and Katarina Bohman (Autoliv Research) for the experimental data on child volunteers and for fruitful discussions. The work was conducted within the SAFER Vehicle and Traffic Safety Centre at Chalmers and at the Indian Institute of Technology, Delhi. Funding for this study was provided by Folksam's Research Fund and the Strategic Area of Advance at Chalmers University of Technology.

VII. References

[1] NHTSA, National Highway Traffic Safety Administration. Child passenger fatalities and injuries, based on restraint use, vehicle type, seat position, and number of vehicles in the crash. Washington, DC: *National Highway Traffic Safety Administration*, US Department of Transportation; 2005. DOT HS 809784

[2] Bidez M. Burke D, King D, Mergl K, Meyer S. A critical safety need for children ages 9-12 in the rear seat. Paper presented at: *Protection of Children in Cars 5th International Conference*; December 6-7, 2007; Munich, Germany

[3] Bohman K, Arbogast K, Bostrom O. Head injury causation scenarios for belted, rear-seated children in frontal impact. *Traffic Injury Prev*. 2011. 12(1):62–70.

[4] van Rooij L, Harkema C, de lange R. de Jager K, Bosch-Rekveldt M, Mooi H. Child poses in child restraints systems related to injury potential: Investigations by virtual testing. Paper presented at: *19th International Technical Conference on the Enhanced Safety of Vehicles* (ESV); June 6–9, 2005; Washington D.C.

[5] Andersson M, Bohman K, Osvalder A-L. Effect of booster seat design on children's choice of seating positions during naturalistic riding. *Annu Proc Ann Adv Automot Med* 2010;54:171-180.

[6] Charlton J, Koppel S, Kopinathan S, Taranto D. How Do Children Really Behave in Restraint Systems While Traveling in Cars? *Annu Proc Assoc Adv Automot Med* 2010;54:181-192.

[7] Jakobsson L, Bohman K, Stockman I, Andersson M, Osvalder A.-L. Older children's sitting postures when riding in the rear seat, *Proc. of International Research Conference on the Biomechanics of Impact* (IRCOBI), Krakow, Poland, September 14–16, 2011.

[8] J. Forman, M. Segui-Gomez, J. Ash, F. Lopez-Valdes, Child posture and shoulder beltfit during extended night-time traveling: an in-transit observational study. *Annu Proc Ann Adv Automot Med.* 2011;55:3-14.

[9] Bohman, K, Stockman, I, Jakobsson, L, Osvalder, A, Boström, O, Arbogast, K. Kinematics and shoulder belt position of child rear seat passengers during vehicle maneuvers. *Annals of Advances in Automotive Medicine*, 2011, 55:15-26.

[10] Beeman SM, Kemper AR, Madigan ML, Franck CT, Loftus SC Occupant Kinematics in Low-speed Frontal Sled Tests: Human Volunteers, Hybrid III ATD, and PMHS. *Accident Analysis and Prevention*. 2012. 47:128–139.

[11] Stockman I, Bohman K, Jakobsson L. Kinematics and shoulder belt position of child anthropomorphic test devices during steering maneuvers. *Traffic Injury Prevention*. 2013. 14:797-806.

[12] Brolin K, Stockman I, Andersson M, Bohman K, Gras LL, Jakobsson L. Safety of children in cars: A review of biomechanical aspects and human body models. *IATSS Research*. 2015. 38:92-102. DOI: 10.1016/j.iatssr.2014.09.001

[13] Östh J, Brolin K, Bråse D. A Human Body Model with Active Muscles for Simulation of Pre-Tensioned Restraints in Autonomous Braking Interventions. *Traffic Injury Prevention*, 2015, 16:304-313.

[14] Cappon H, Mordaka J, van Rooij L, Adamec J, Praxl N, Muggenthaler H. A computational human model with stabilizing spine: a step towards active safety. *SAE Technical paper* no 2007-01-1171, 2007.

[15] MADYMO Human Models Manual Release 7.4.1. TASS, Rijswijk, the Netherlands, 2012.

[16] Stockman I, Bohman K, Brolin K, Jakobsson L. Kinematics of Child Volunteers and Child Anthropomorphic Test Devices During Emergency Braking Events in Real Car Environment. *Traffic Injury Prevention*, 2013, 14:92-102.

[17] De Faveri E. Kinematics and shoulder belt position of child volunteers when exposed to steering manoeuvres in different restraint systems. Master's Thesis 2013:35, *Chalmers University of Technology*, Gothenburg, Sweden, 2013. http://publications.lib.chalmers.se/records/fulltext/185323/185323.pdf

[18] Andersson M, Pipkorn B, Lövsund P. Evaluation of the Head Kinematics of the Q3 Model and a Modified Q3 Model by Means of Crash Reconstruction. *Traffic Injury Prevention.* 2012. 13:600–611.

[19] de Vlugt E, Schouten AC, van der Helm FCT. Quantification of Intrinsic and Reflexive Properties during Multijoint Arm Posture. *Journal of Neuroscience Methods* 2006. 155:328–349.

[20] Forbes PA, Siegmund GP, Schouten AC, Blouin J-S. Task, Muscle, Frequency Dependent Vestibular Control of Posture. *Frontiers in Integrative Neuroscience.* 2015. 8:94.

[21] de Bruijn. Isometric and Dynamic Motor Control of Neck Muscles. Ph.D. Thesis: *Delft University of Technology*, Delft, the Netherlands. 2014.

[22] Massion J. Movement, Posture and Equilibrium: Interaction and Coordination. *Progress in Neurobiology* 1992. 38:35–56.

[23] Meijer R, Broos J, Elrofai H, de Bruijn E, Forbes P, Happee R. Modelling of Bracing in a Multi-Body Active Human Model. *Proceedings of the IRCOBI Conference*; Gothenburg, Sweden. 2013.

[24] Iwamoto M, Nakahira Y, Kimpara H, Sugiyama T. Development of a Human Body Finite Element Model with Multiple Muscles and their Controller for Estimating Occupant Motions and Impact Responses in Frontal Crash Situations. *Stapp Car Crash Journal.* 2012. 56:231–268.

[25] Zajac FE. Muscle and Tendon: Properties, Models, Scaling, and Application to Biomechanics and Motor Control. *Critical Reviews in Biomedical Engineering*. 1989, 17(4):359–410.

[26] Fraga F, van Rooj L, Symeonidis I, Peldschus S, Happee R, Wismans J (2009) Development and Preliminary Validation of a Motorcycle Rider Model with Focus on Head and Neck Biofidelity, Recurring to Line Element Muscle Models and Feedback Control. *Proceedings of the 21st ESV Conference*; Stuttgart, Germany.